RESEARCH

Recombinant *Lactococcus lactis* secreting FliC protein nanobodies for resistance against *Salmonella* enteritidis invasion in the intestinal tract

Ming Yang[1,2†], Kui Gu[3†], Qiang Xu[1,2†], Renqiao Wen[1,2], Jinpeng Li[1,2], Changyu Zhou[1,2], Yu Zhao[1,2], Miwan Shi[3], Yuan Weng[3], Boyan Guo[1,2], Changwei Lei[1,2], Yong Sun[4] and Hongning Wang[1,2*]

Abstract

Salmonella Enteritidis is a major foodborne pathogen throughout the world and the increase in antibiotic resistance of *Salmonella* poses a significant threat to public safety. Natural nanobodies exhibit high affinity, thermal stability, ease of production, and notably higher diversity, making them widely applicable for the treatment of viral and bacterial infections. Recombinant expression using *Lactococcus lactis* leverages both acid resistance and mucosal colonization properties of these bacteria, allowing the effective expression of exogenous proteins for therapeutic effects. In this study, nine specific nanobodies against the flagellar protein FliC were identified and expressed. In vitro experiments demonstrated that FliC-Nb-76 effectively inhibited the motility of *S*. Enteritidis and inhibited its adhesion to and invasion of HIEC-6, RAW264.7, and chicken intestinal epithelial cells. Additionally, a recombinant *L. lactis* strain secreting the nanobody, *L. lactis*-Nb76, was obtained. Animal experiments confirmed that it could significantly reduce the mortality rates of chickens infected with *S*. Enteritidis, together with alleviating the inflammatory response caused by the pathogen. These results provide a novel strategy for the treatment of antibiotic-resistant *S*. Enteritidis infection in the intestinal tract.

Keywords *S*. Enteritidis, Recombinant *Lactococcus lactis*, FliC protein nanobodies, Targeted bacteriostasis

Introduction

Salmonella Enteritidis is one of the most harmful *Salmonella* serotypes and is estimated to cause 1.35 million infections, 26 500 hospitalizations, and 420 deaths each year in the USA, posing a serious threat to public safety [1, 2]. Antibiotics are usually used for treating bacterial infections, and β-lactam antibiotics, including third-generation cephalosporins, as well as aminoglycosides and fluoroquinolones, are commonly used for the treatment of *Salmonella* infections. However, the development of antibiotic resistance together with other issues poses significant challenges to clinical treatment [3, 4]. A recent
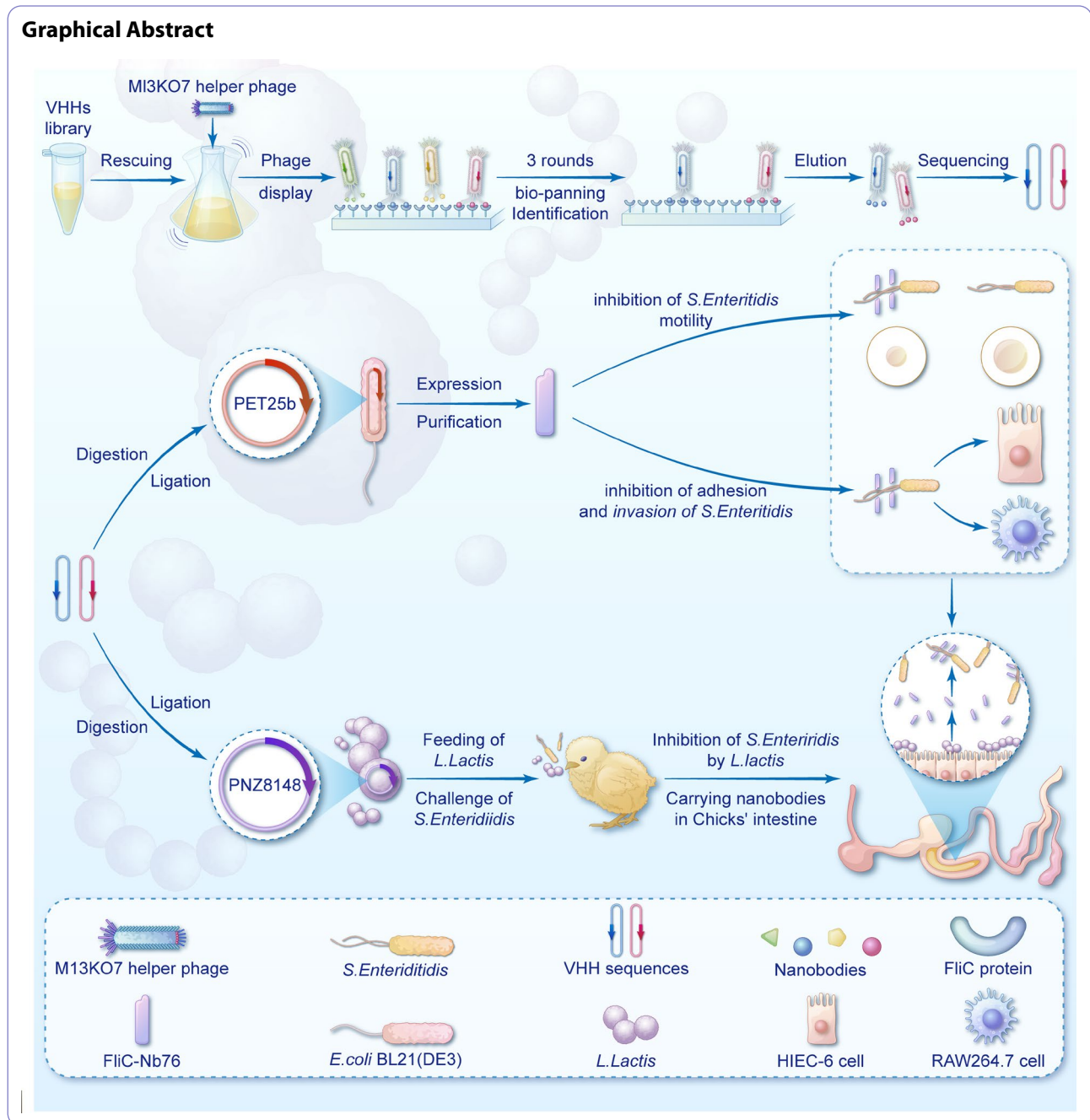
†Ming Yang, Kui Gu and Qiang Xu contributed equally to this work.

*Correspondence:
Hongning Wang
whongning@163.com

Full list of author information is available at the end of the article

Graphical Abstract

study found that 36,822 *Salmonella* isolates showed resistance to 15 commonly used antibiotics, with 7.2% of the strains resistant to only one antibiotic and 66.5% exhibiting multidrug resistance, a high degree of resistance (73.4%) to ampicillin was observed among the isolated strains [5]. Therefore, the timely development and exploration of alternatives to antibiotics and other therapeutic strategies are important directions for the future treatment of *Salmonella* infections [6–8].

Nanobodies (Nbs) are genetically engineered antibodies that contain only the heavy chain variable region

(VHH). Compared with conventional IgG antibody molecules (150 kDa), nanobodies are characterized by having low molecular weight, no Fc terminal, intact antigen-recognition ability, high solubility and penetration, and are relatively easy to produce, express, and modify [9]. In addition, nanobodies, like traditional antibodies, are able to neutralize both viruses [10–12] and pathogenic bacteria infecting host cells [13–16]. Specific nanobodies developed against the *Shigella* invasion plasmid antigen D (IpaD) were found to reduce *Shigella* infection, and modified VHH heterodimers could reduce

Yang *et al. Journal of Nanobiotechnology*   (2024) 22:629

Page 3 of 16

hemolysis induced by *Shigella* by 80% [17]. Nanobodies against *Vibrio cholerae* lipopolysaccharides were effective in neutralizing *V. cholerae* infection in vitro, while oral administration of the nanobodies effectively reduced cholera symptoms in mice [18]. Specific nanobodies targeting conserved regions of the outer membrane proteins of *Campylobacter jejuni* and *C. coli* were able to control *C. jejuni* colonization in the chicken gastrointestinal tract [19]. These studies suggest that the development of nanobodies against surface components and virulence proteins of specific pathogens can prevent pathogen infection, and this form of nanobody therapy may be a new alternative to antibiotic treatment.

The *Salmonella* FliC protein functions as a virulence factor and constitutes the major protein component of the flagellar apparatus, an assembly of flagellate-like filaments responsible for *Salmonella* motility [20, 21]. At the same time, the flagellar locomotor apparatus of *Salmonella* contributes to the attachment of the bacterium to host cells, facilitating the invasion process [22, 23]. A study by Riazi et al. [24] used *C. jejuni* flagellin to immunize llamas to obtain a 5×10^7 PFU phage display library followed by transformation of selected nanobodies into pentamers by genetic engineering; it was found that the pentameric nanobodies reduced motility and colonization of *C. jejuni* in the chicken intestine.

While the use of nanobodies has significant potential in the treatment of infection, they also have several drawbacks. Their small size and low molecular weight (approximately 15 kDa) contribute to a short half-life with rapid clearance by the kidneys when used in vivo; in addition, the maintenance of therapeutic drug concentrations over extended periods is challenging [25]. In most cases, additional modifications are required before use. *Lactococcus lactis* is commonly used in the preparation of cheese, drinks, and meat and is a safe microorganism [26], it produces lactic acid through fermentation and is resistant to the harsh environment of the gastrointestinal tract, maintaining the activity of its enzymes. *L. lactis* is also used as a probiotic and can colonize the intestinal mucosa, competing with pathogenic microorganisms for its ecological niche and thus reducing pathogen colonization. In addition, *L. lactis* can express foreign proteins by means of the Nisin-induced gene expression (NICE) system. Thus, recombinant expression of *L. lactis* can not only resist the acid intestinal environment and prevent pathogen colonization but can also express foreign proteins [27, 28] and can be used as an oral delivery carrier for biological drugs [29].

As shown in Scheme 1 in this study, the effects of FliC-Nb76 on the neutralization of *S.* Enteritidis were assessed at the cellular level. The nanobodies not only neutralized antibiotic-sensitive *S.* Enteritidis, but also neutralized multidrug-resistant *S.* Enteritidis. This is the first report of the use of *L. lactis* for the expression and delivery of neutralizing nanobodies against the FliC protein. The inhibitory effects of anti-FliC-expressing *L. lactis* on the colonization of *S.* Enteritidis in chick intestinal tracts were evaluated and a strategy for the delivery of nanobodies to the intestinal tract was proposed, providing a novel treatment for *S.* Enteritidis infection in the intestinal tract of chicks.

Materials and methods
Materials and reagents
Freund's adjuvant (complete and incomplete) was purchased from Sigma Aldrich (St Louis, MO, USA). All restriction enzymes used in the study were from New England Biolabs (Ipswich, MA, USA). The double blood bags used for blood collection were purchased from Suzhou Leishi Blood Transfusion Equipment Co., Ltd. (Suzhou, China) and 96-well microplates were obtained from Corning (Corning, NY, USA). Kits, including kits for PCR purification, gel extraction, and the TIANprep Mini Plasmid Kit for plasmid preparation were purchased from Tiangen (Beijing, China). Chloramphenicol (Chl), ampicillin, kanamycin, isopropyl-β-d-thiogalactoside (IPTG), the Ni-IDA 6FF His tag protein purification kit, Ni-IDA/Ni-NTA elution buffer, and Ni-IDA/Ni-NTA binding/wash buffer were purchased from Sangon Biotech (Shanghai, China). Unless otherwise noted, all reagents used in the study were of analytical grade. Details of the primers used in the study are provided in the supporting information.

Cells, strains, and vectors
The RAW264.7 cell line was cultured in Dulbecco's Modified Eagle Medium (DMEM, Life Technologies, Carlsbad, CA, USA) supplemented with 10% fetal bovine serum (FBS, Gibco, Waltham, MA, USA). The HIEC-6 cell line was cultured in HIEC-6 complete culture medium (MeisenCTCC, China). All the bacterial strains used had been preserved in our laboratory (Animal Disease Prevention and Food Safety Key Laboratory of Sichuan Province, Chengdu, China) including *E. coli* TG1, *S.* Enteritidis FY-04, *S.* Enteritidis ATCC 13,076 (GenBank accession JAKIRO000000000) and Clinical isolates *S.* Enteritidis ZZ64, *S.* Enteritidis ZZ77, *S.* Enteritidis ZZ80, *S.* Enteritidis ZZ82. The *S.* Enteritidis FliC protein was expressed in an *E. coli* system using pET-28a vector (Novagen, USA). Recombinant nanobody fusions against the FliC protein were expressed in an *E. coli* system using the pET-25b vector (Novagen, USA). The pMECS vector and M13KO7 helper phage were preserved in our laboratory and were used to construct the VHH library.

Preparation of FliC protein

The full-length gene primers were designed based on the reference sequence of the FliC protein (1518 bp) (Gen-Bank: Z15068.1) and its theoretical molecular weight is about 60 kDa (including the tag sequence on the plasmid). The FliC protein gene was cloned into the PET28a vector and transformed into BL21 (DE3) competent cells. Positive transformants were induced using IPTG at a final concentration of 0.5 mM for 8 h at 16℃. The recombinant FliC protein was analyzed by SDS-PAGE and Western blotting, and performed grayscale scanning on imageJ to determine its purity.

Screening and identification of specific anti-FliC protein nanobodies

The VHH library used in this study was derived from previously constructed and stored sources [30]. Nanobodies specifically recognizing the FliC protein were selected in three rounds of bio-panning, as described previously [24, 27]. The 200 μL VHH library was cultured in 2 × TY medium until growth reached the logarithmic phase and was infected with M13KO7 helper phage to obtain the rescue phage. The FliC protein was used to coat 96-well plates (20, 10, and 5 μg/well from the first to the third rounds of panning) at 4℃ overnight. The coated wells were washed three times with PBS containing 2% (v/v) Tween-20 (PBST), and then blocked with 3% skimmed milk (w/v) for 1 h. Rescue phages (5×10^{11} PFU) were then added and incubated at 37℃ for 1 h. Each well was then washed 15 times with PBST, before the addition of 100 μL of 100 mM triethylamine, pH=11.0 (TEA), and incubation for 10 min at room temperature, after which the specific phage particles were eluted and immediately neutralized with 100 μL 1.0 mM Tris/HCl (pH=7.4). Subsequently, for the next round of selection, the eluted phage particles were used to infect TG1 cells for the evaluation of titration and amplification. The infected TG1 cells were counted to quantify the input and output of the phages, and the enriched phage particles were detected using indirect ELISA (iELISA) with an anti-M13 antibody (Hangzhou Hua'an Biotechnology Co., Ltd., Hangzhou, China). After three rounds of screening, 96 clones were randomly selected from the phage eluted in the third round. After induction with 1 mM IPTG after growth to the logarithmic phase in TB medium, the soluble nanobodies were expressed in the periplasm of *E. coli* in 96-well plates. Multiple freeze-thaw cycles were used to yield the periplasmic extract (PE), consisting of nanobodies with hemagglutinin (HA) and His tags. In addition, the presence of specific anti-FliC nanobodies was determined using an iELISA with a mouse anti-HA monoclonal antibody (Beijing Zhonghua Biotechnology Co. Ltd., China). Finally, the positive colonies (P/N>3.0) were identified and classified by sequencing and of the amino acid sequences of complementary determining regions (CDRs).

Expression, purification, and characterization of the FliC-Nbs

The prokaryotic expression system was designed according to the VHH sequences of the FliC protein. The FliC-Nb genes were cloned into the PET25b vector to yield the PET25b-FliC-Nb recombinant plasmid. The expression and purification of the FliC-Nbs were analyzed by SDS-PAGE. The binding and specificities of the purified nanobodies against the FliC protein and *S.* Enteritidis were confirmed by iELISA using an anti-HSV tag monoclonal antibody for detection. The concentration of FliC protein is 4 μg/mL, the concentration of S. Enteritidis is 1×10^{8} CFU/mL, the concentration of nanobodies is 1 μg/mL, the dilution ratio of mouse anti HSV monoclonal antibody is 1:3000, and the dilution ratio of HRP goat anti mouse IgG antibody is 1:4000.

Prediction and analysis of the binding sites between the FliC protein and FliC-Nbs

The reference sequence of the *S.* Enteritidis FliC protein (Z15068.1) was downloaded from GenBank and converted into an amino acid sequence. Based on the amino acid sequence of FliC-Nbs, the corresponding.pdb file was downloaded from the Protein Data Bank database or analyzed using the SWISS-MODEL online software to search for templates that were then used for structure modeling. ClusPro was used for docking FliC-Nbs and the FliC protein, with the top-ranked docking pose considered the binding conformation. The docked structures were visualized in PyMol and binding affinities were analyzed using PDBePISA online software. Ligplot 2.2.4 was employed to analyze the binding mode (interactions) between the antigen and the antibody.

Expression and characterization of EGFP-FliC-Nbs and the binding between S. Enteritidis and EGFP-FliC-Nbs

The FliC-Nbs were cloned into the PET22b-EGFP vector with EGFP protein expression at the C-terminus of nanobodies and their expression and purity were analyzed using SDS-PAGE and Western blotting. Binding of the EGFP-FliC-Nbs to mCherry *S.* Enteritidis in the logarithmic growth phase was observed using confocal laser scanning microscopy with different excitation light sources.

FliC-Nbs inhibit the motility of *S.* Enteritidis

Flagella are the motor organs of bacteria, controlling their motility as well as facilitating bacterial adhesion and invasion [31]. During the initial phase of gastrointestinal colonization, *Salmonella* utilizes flagella-mediated locomotion to reach its preferred site of infection

[32]. The effects of the FliC-Nbs on *S.* Enteritidis motility were, therefore, examined. *S.* Enteritidis was cultured until reaching logarithmic growth, after which a suspension containing 5×10^6 CFU was mixed with 0.5 mg/mL of FliC-Nbs (using BSA as the control). After incubation for 30 min at 37℃, 1 μL of the *S.* Enteritidis suspension was dropped vertically into the center of a 0.4% solid agar-LB plate and incubated at 37℃ for 6 h. The diameter of the diffusion circle was measured and the area of diffusion was calculated. *S.* Enteritidis was incubated with FliC-Nbs for 30 min at 37 °C, with BSA used as a control, and morphological changes in the flagella of *S.* Enteritidis were observed under transmission electron microscopy. To verify whether the FliC-Nbs could inhibit the motility of other clinical *S.* Enteritidis isolates, the same procedure was followed with *S.* Enteritidis, to determine the inhibitory effects of FliC-Nbs on the motility of four clinical isolates of *S.* Enteritidis (ZZ64, ZZ77, ZZ80, and ZZ82). To explore the concentration of FliC-Nbs most effective for inhibiting *S.* Enteritidis motility, *S.* Enteritidis was pretreated with 0.4, 0.2, 0.1, and 0.05 mg/mL FliC-Nbs, and the same method was used to observe and record the movements of *S.* Enteritidis. The lowest effective concentration was defined as that which produced significant inhibition of the circling movements of *S.* Enteritidis relative to the control group. The effects of the minimum effective concentration of FliC-Nbs (using BSA as the control) on the motility of mCherry *S.* Enteritidis was observed under confocal laser scanning microscopy and the inhibitory effects of the FliC-Nbs was determined by observing the distance traveled within a specified time frame.

Inhibition of *S.* Enteritidis infection of HIEC-6 and RAW264.7 cells by FliC-Nbs

Invasion of intestinal epithelial cells by *S.* Enteritidis is the precondition of intestinal infection, and the ability of the bacteria to replicate in macrophages is key to the establishment of systemic infection. Therefore, we selected normal human intestinal epithelial cells (HIEC-6) and mouse macrophage leukemia cells (RAW264.7) for further experiments. The infection of both HIEC-6 and RAW264.7 cells by *S.* Enteritidis can be divided into two stages, namely, adhesion and invasion. mCherry *S.* Enteritidis (ATCC13076) in the logarithmic growth phase were mixed with 0.5 mg/mL FliC-Nbs for 30 min. Both cell lines were incubated using a multiplicity of infection (MOI) of 50. After treatment for 1 h, unabsorbed *S.* Enteritidis were discarded and the cells were washed three times with PBS to evaluate the effects of FliC-Nbs on *S.* Enteritidis adhesion to the cells. Five wells of HIEC-6 cells were treated with 1% Triton X-100 for 10 min to induce lysis, with the lysates recorded as "*S.* Enteritidis adhesion", while cells in the remaining wells were fixed with 0.4% paraformaldehyde for 15 min and evaluated under fluorescence microscopy (Leica Microsystems, Germany). The adhesion of mCherry *S.* Enteritidis to the cells was assessed by integrated optical density analysis with ImageJ software. Five wells of infected cells were cultured in medium containing 100 μg/mL of gentamicin (a non-membrane-permeable antibiotic that kills non-internalizing bacteria) for 1 h, after which the cells were washed three times with PBS. Then the wells were treated with 1% Triton X-100 for 10 min and the lysate was collected and labeled "*S.* Enteritidis invasion". The collected lysates were then serially diluted and the numbers of *S.* Enteritidis were counted. Camel serum after five immunizations was used as the PS (positive serum) group, while the NS (negative serum) group consisted of serum without specific antibodies, all serum were used after being diluted at a 1:1000 ratio. The rates of adhesion and invasion inhibition were calculated as: (bacterial count in the infected group − the bacterial count in the other experimental treatment groups/bacterial count in the infected group) × 100%. Additionally, to confirm the inhibitory effects of FliC-Nb7s on other clinically isolated multidrug-resistant strains of *S.* Enteritidis, the mCherry-ZZ64 and mCherry-ZZ77 strains were used as test strains. The same procedure was used to verify the neutralizing effects of FliC-Nbs, focusing on its impact on these strains.

Inhibition of *S.* Enteritidis infection of chick intestinal epithelial cells by FliC-Nbs

Five healthy chicks of uniform size and weight were sacrificed. The jejunum was removed, washed three times with PBS containing 50 μg/mL of gentamicin (PBS-G), and cut into 1.5 cm segments. Each segment was placed in a well of a 24-well cell culture plate containing 1 mL DMEM (with 50 μg/mL gentamicin) and incubated at 37℃ for 1 h. *S.* Enteritidis FY-04 grown to the logarithmic phase ($OD_{600}=0.5$) were mixed with 0.5 mg/mL of FliC-Nb76. The negative control group comprised PBS and BSA. The mixture was incubated at 37℃ for 30 min. The treated *S.* Enteritidis FY-04 were then inoculated into each well, with a seeding amount of 1×10^8 CFU per well and 500 μL of DMEM and incubated for 1 h. After a 15-minute static incubation with PBS-G, non-adherent *S.* Enteritidis were removed. The jejunal segments were then washed three times with PBS and 1 mL of DMEM was added for another 1-h incubation, then washed three times with PBS, and total DNA was extracted from each segment. qPCR reactions were performed using the primers qPCR-SE-F and qPCR-SE-R on a 10-fold diluted PMD18-T-HilA plasmid template. A standard curve for qPCR detection was constructed using the logarithmic copy number of the PMD18-T-HilA plasmid to evaluate

the targeted inhibitory effect of FliC-Nb76 on *S.* Enteritidis infection in chick intestinal epithelial cells.

Preparation, induced expression, and identification of recombinant *L. lactis-* secreting nanobodies

The signal peptide sequence of the *L. lactis* secretion peptide USP45 (MKKKIISAILMSTVILSAAAPLSGVYA), the secretion peptide enhancement sequence (LEISSTCDA), FliC-Nbs and the 6×His tag sequences were sequentially linked and sent to Sangon Biotech (Shanghai) for synthesis, after which they were constructed into the PUC57 plasmid to yield the recombinant plasmid PUC57-USP45-LEISSTCDA-FliC-Nbs. A homologous recombination method was used to construct the fusion gene sequence of the nanobody into the PNZ8148 plasmid, which was then transformed into MC1061F-competent cells to yield the recombinant plasmid PNZ8148-USP45-LEISSTCDA-FliC-Nbs. The recombinant plasmid was electroporated into *L. lactis* NZ9000 competent cells to obtain PNZ8148-USP45-LEISSTCDA-FliC-Nbs-*L. lactis* NZ9000 (FliC-Nbs-NZ9000), referred to hereafter as *L. lactis*-VHH. An overnight culture of the recombinant *L. lactis*-VHH was transferred to 20 mL of M17B/Chl medium at a ratio of 1:50. After addition of Nisin at a final concentration of 20 ng/mL to induce expression, the supernatant was collected. The fusion His-tagged protein secreted in the supernatant was identified using western blotting. The bacterial pellet was washed twice with PBS, and the bacterial cells were used for whole-cell ELISA to detect the fusion His-tagged antibody [33]. The recombinant *L. lactis*-VHH cultured overnight was transferred to 20 mL M17B/Chl medium at the ratio of 1:50 and grown until reaching the logarithmic growth stage (OD_{600}=0.6). At the same time, 1 mL samples of culture supernatant were collected at 2, 4, 6, 8, 10, and 12-h time points to detect the fusion His-tagged nanobody using western blotting, to determine the optimal induction time. Additionally, the expression level of the secreted nanobody in the culture supernatant was accurately measured using a His tag ELISA kit. Following the protocol of previous studies [34], one hour after Nisin induction, the pellet was resuspended in 20 mL of M17B/Chl medium and culture was continued for a further 12 h, together with an uninduced bacterial culture as a control. Samples of the culture supernatants were collected every 2 h and centrifuged, and the expression of the fusion His-tagged nanobody was determined using

western blotting. The concentration of recombinant nanobodies expressed by FliC-Nb76-NZ9000 strain was determined using His Tag competitive ELISA kit. The aim was to explore the effect on the expression of removing the inducer. The ability of the nanobody secreted by *L. lactis*-VHH to recognize *S.* Enteritidis was determined using iELISA.

Detection of targeted inhibition of *S.* Enteritidis in the intestinal tracts of chicks by *L. lactis*-secreting nanobodies

Sixty-week-old chicks were divided into four groups with 15 chicks per group. The groups were the SE, PBS, PNZ8148-NZ9000, and FliC-Nbs-NZ9000 groups (Table 1). For the preparation of the *S.* Enteritidis mixture, *S.* Enteritidis FY-04, *S.* Enteritidis SE (ZZ64), and *S.* Enteritidis (ZZ76) were cultured to the logarithmic stage, with adjustments of the concentrations of the bacterial solutions to 2×10^{9}CFU/mL. The same volume of the concentration of *S.* Enteritidis was mixed and configured into 2×10^{9} CFU/mL of three kinds of *S.* Enteritidis mixture. For the preparation of the *L. lactis*-VHH mixture, the concentration of PNZ8148-NZ9000 and FliC-Nbs-NZ9000 after removal of Nisin was adjusted to 1×10^{10} CFU/mL. All groups were fed samples for three days and apart from the PBS group, the remaining groups were given 1 mL of a mixture of *S.* Enteritidis on day 3 of feeding. Feces were collected on days 3 and 7 of the challenge and were weighed and resuspended in PBS at a mass: volume ratio of 1:10, and the colonies were counted on XLT4 Agar- ampicillin-resistant plates following gradient dilution. Total DNA was extracted from the duodenum, jejunum, and ileum of the chicks on days 3 and 7, and the copy numbers of specific *S.* Enteritidis genomes in the intestine were determined by qPCR using the method described above. On day 7, the intestines of chicks from the different groups were excised and examined by live imaging, while ileal samples were collected and fixed with 4% paraformaldehyde for the preparation of tissue sections. The sections were stained with HE, and the tissue structure and cell morphology were observed under the microscope (Leica Microsystems, Germany). Additional duodenal, jejunal, and ileal samples collected on day 7 were ground with liquid nitrogen and total RNA was extracted using TRIzol. The mRNA expression levels of the inflammatory cytokines TNF-α, IL-8, IL-17 A, IL-10, and IL-1β were determined by qPCR with GAPDH used as an internal reference and the relative mRNA expression levels were calculated by the $2^{\wedge(\triangle\triangle CT)}$ method. The reaction conditions and reaction system were as described above.

Statistical analysis
All the assays were independently repeated at least three times. Data were analyzed using GraphPad Prism version

Table 1 Classification of *S.* Enteritidis challenge

Group	Samples	Dosage
PBS	PBS	1mL
SE	PBS	1mL
PNZ8148-NZ9000	1×10^{10} CFU/mL PNZ8148-NZ9000	1mL
FilC-Nb76-NZ9000	1×10^{10} CFU/mL FilC-Nb76-NZ9000	1mL

9.0 (GraphPad Software, San Diego, CA, USA) using a one-way analysis of variance (one-way ANOVA) followed by Tukey's post hoc tests, comparing all pairs of columns. P-values < 0.05 were considered statistically significant.

Results

Expression and purification of the FliC protein, and screening and characterization of anti-FliC nanobodies

The scheme of the screening process is shown in Fig. 1A. The FliC gene (1518 bp) was successfully ligated into the pET-28a (+) vector (Fig. 1B). Analysis of the protein on SDS-PAGE showed that compared to the empty vector control strain, the FliC protein-expressing strain showed an additional protein band at ~60 kDa (Fig. 1C), corresponding to the expected molecular weight of FliC.

After ultrasonic disruption and purification using a nickel column, performing grayscale scanning on imageJ to determine its purity, a single purified protein band was obtained with a purity exceeding 95% (Fig. 1D). The presence of the recombinant protein with a His tag was confirmed by Western blotting using a monoclonal antibody specific for the His tag (Fig. 1E). A noticeable upward trend in the titer of the phage particles against FliC protein-specific nanobodies was observed after three consecutive rounds of bio-panning, with the output increasing from 6.8×10^4 PFU in the first round to 7.5×10^7 PFU in the third round. Concurrently, the proportion of specific phage also rose from 12.6 to 5.35×10^2 (Table 2). The overall findings suggested the effective enrichment of specific phages against the FliC protein
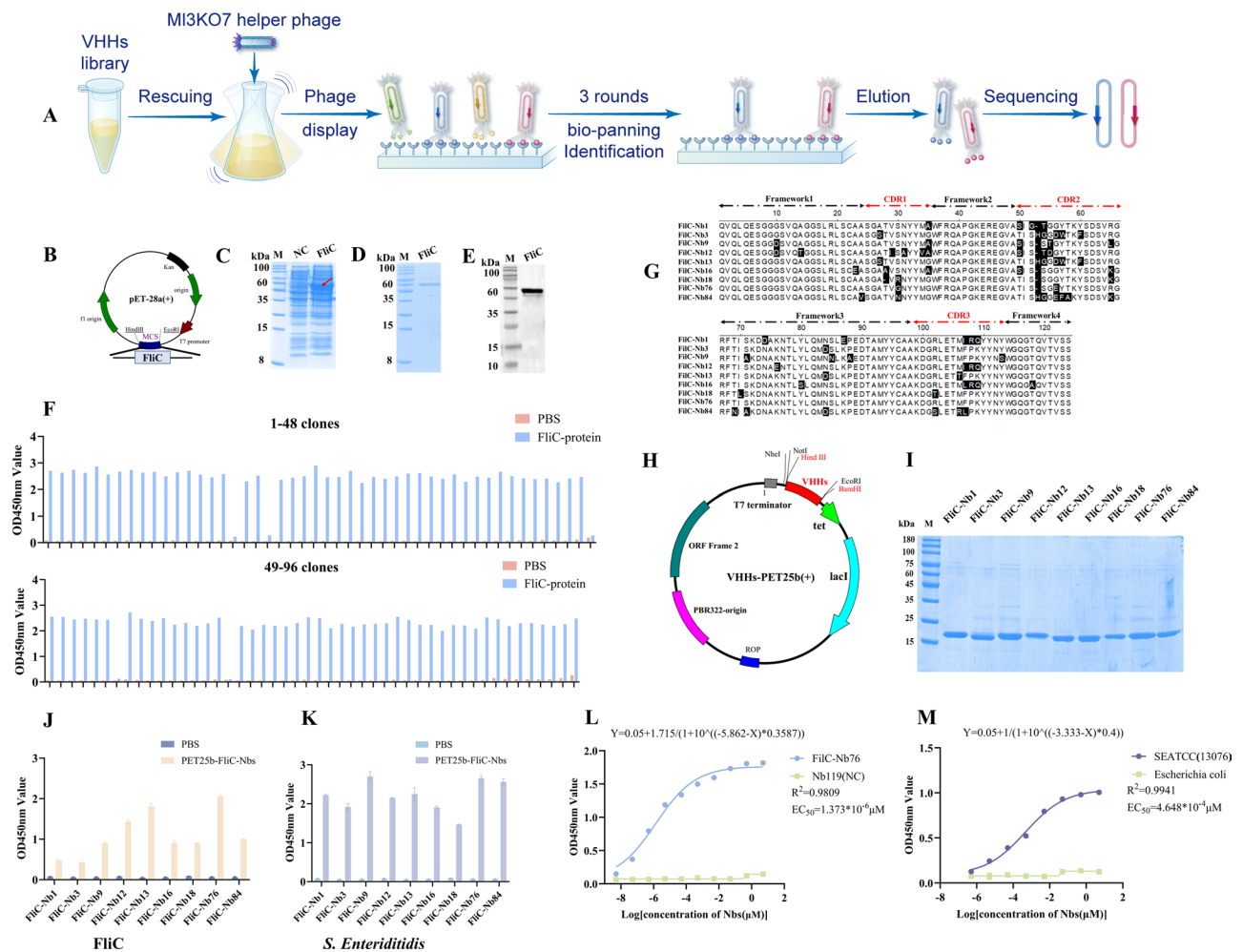

Fig. 1 Expression, purification of FliC protein, screening, expression, and characterization of nanobodies against FliC protein. **A** Scheme of screening for nanobodies against FliC protein. **B** Graphical representation of pET-28a (+)-FliC protein construction. **C** Comparison of FliC protein expression to the empty vector by SDS-PAGE. **D** Analysis of FliC protein purification by SDS-PAGE. **E** Determination FliC protein by Western blot. **F** Identification the periplasmic extract of 96 clones to specifically bound with the FliC protein, with positive rate of 94.8% (91/96), and the PBS protein is employed as the negative control. **G** Alignment and classification of the amino acid sequences of 9 screened nanobodies based on CDRs. **H** Construction of prokaryotic expression plasmid of FliC-Nbs. **I** Expression of FliC-Nbs were induced by IPTG. Purification of FliC-Nbs with Ni-IDA 6FF. **J** ELISA identification of FliC-Nbs with FliC protein. **K** ELISA identification of FliC-Nbs with *S.* Enteritidis FY-04. **L** EC$_{50}$ curve for FliC protein binding by FliC-Nb76. **M** EC$_{50}$ curve for FliC *S.* Enteritidis binding by FliC-Nb76

Table 2 Enrichment of phage particles against FliC protein specific nanobodies during three rounds of panning

Round of screening	Input (PFU/well)	P output (PFU/well)	N output (PFU/well)	Recovery (P/Input)	P/N
1st Round	5×10^{11}	6.8×10^4	5.4×10^3	1.36×10^{-8}	12.6
2nd Round	5×10^{11}	8.8×10^5	2.8×10^4	1.76×10^{-6}	31.4
3rd Round	5×10^{11}	7.5×10^7	1.4×10^5	1.5×10^{-4}	5.35×10^2

during the screening process. Ninety-six clones selected from the elution titer-determination plates in the third round of bio-panning were analyzed by ELISA using the induced bacterial periplasmic extracts, which showed that 91 clones were positive ($P/N \geq 3.0$), yielding a positivity rate of 94.8% (91/96) (Fig. 1F). Classification based on the CDRs of the VHH amino acid sequences identified nine distinct nanobodies, designated as FliC-Nb1, FliC-Nb3, FliC-Nb9, FliC-Nb12, FliC-Nb13, FliC-Nb16, FliC-Nb18, FliC-Nb76, and FliC-Nb84 (Fig. 1G). These findings demonstrated the successful screening of nine nanobody sequences against the FliC protein. The selected nanobody genes were ligated into the PET25-b vector (Fig. 1H). Successful expression of the VHH antibodies was observed after 16 h of induction with 0.2 mM IPTG. All the target proteins had molecular weights of approximately 20 kDa (nanobodies and tag protein) and were all soluble, SDS-PAGE showed a single protein band with a purity of over 95% (Fig. 1I). The ability of the recombinant nanobodies expressed in the prokaryotic expression system to recognize FliC protein was verified by ELISA, with the ELISA results showing that nine strains of FliC-Nbs could recognize FliC protein (Fig. 1J) and *S.* Enteritidis (Fig. 1K). Preliminary plate migration experiments showed that FliC-Nb-76 had the most significant inhibitory effect on *S.* Enteritidis motility, so this antibody was chosen for subsequent experiments (Fig. S1). The EC_{50} values were determined under coating conditions where the concentration of FliC protein was 4 µg/mL and the concentration of *S.* Enteritidis was 1×10^8 CFU/mL. The EC_{50} of Nb76 against FliC was determined to be 1.373×10^{-6} µM (Fig. 1L), while against *S.* Enteritidis, the EC_{50} was found to be 4.648×10^{-4} µM (Fig. 1M).

FliC-Nb76 binding to *S.* Enteritidis and inhibition of its motility

Searched and downloaded the protein structure PDB file for the *S.* Enteritidis FliC protein from the official PDB database website (PDB ID: Q06972). The amino acid sequence comparison revealed no discrepancies between the sequence and the target amino acid sequence. Using SWISS-MODEL online software to perform homology modeling based on the FliC-Nb76 amino acid sequence, the template with the highest score was obtained for modeling (Figure S2), and the protein PDB file with the

highest score was selected for download; Using CLUS-PRO with FliC-Nb76 nanobody as the receptor and FliC protein as the ligand, docking is performed in antibody mode, and the highest ranked docking conformation output is considered the binding conformation. The docking results were visualized using PyMol, with the binding region shown in yellow (Fig. 2A). Ligplot 2.2.4 was utilized to analyze the binding mode (interactions) between FliC-Nb76 and the FliC protein (Fig. 2B). In the structure, chain A represents the FliC protein, while chain B represents FliC-Nb76. The primary interactions involved in the binding were found to be hydrogen bonds and hydrophobic interactions, which revealed the potential molecular binding mechanism and provides a model for the subsequent design of related drugs. Successful expression of EGFP-FliC-Nb76 (Fig. 2C) was confirmed using SDS-PAGE (Fig. 2D) and Western blotting (Fig. 2E). The pFPV-mCherry plasmid was successfully transformed into *S.* Enteritidis (Figure S3), and binding between the mCherry *S.* Enteritidis and green fluorescent-labeled EGFP-FliC-Nb76 was observed under confocal laser scanning microscopy (Fig. 2F). Compared to the BSA control group, FliC-Nb76 was found to significantly reduce the motility area of *S.* Enteritidis FY-04 on 0.4% agar plates (Fig. 2G). Electron microscopy observations showed that the flagellar morphology of *S.* Enteritidis FY-04 was normal after treatment with BSA but was altered after treatment with FliC-Nb76, with some flagella showing clustering and entanglement (Fig. 2H). To explore the inhibitory effects on clinical isolates of drug-resistant *S.* Enteritidis using the same method, and the results showed that FliC-Nb76 significantly reduced movement of the *S.* Enteritidis strains ZZ64, ZZ77, ZZ80, and ZZ82 on 0.4% agar plates. Investigation of the minimum inhibitory concentration of FliC-Nb76 (Fig. 2I) showed that when the concentration of FliC-Nb76 was 0.1 mg/mL, there was no significant difference relative to the group treated with BSA. When the concentration of FliC-Nb76 was 0.2 mg/mL, the area of movement of *S.* Enteritidis was significantly less than that in bacteria treated with BSA ($P < 0.05$) (Fig. 2J), indicating that the minimum inhibitory concentration of FliC-Nb76 was 0.2 mg/mL. Under confocal laser scanning microscopy, *S.* Enteritidis FY-04 treated with BSA exhibited normal motility with rapid movement, whereas the motility of *S.* Enteritidis FY-04 treated with FliC-Nb76 was significantly inhibited, with almost no movement (Fig. 2K). The distance traveled by *S.* Enteritidis FY-04 after treatment with BSA was much greater than that of *S.* Enteritidis FY-04 treated with FliC-Nb76 (Fig. 2L).
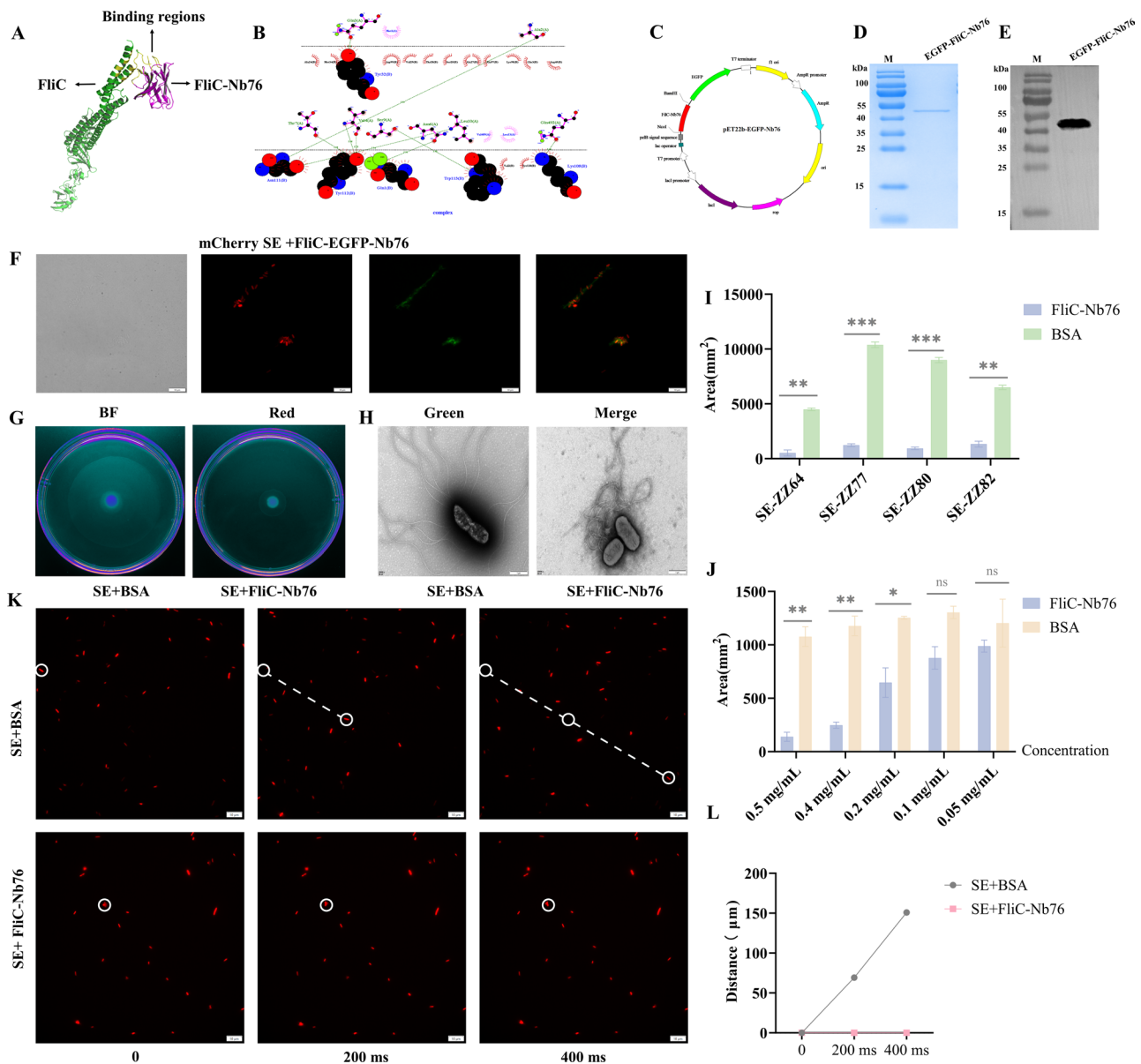
Fig. 2 FliC-76 binding to *S.* Enteritidis and inhibition of its motility. **A** Binding conformation between FliC-Nb76 with FliC protein and the yellow areas are the Binding regions. **B** Two-dimensional graphics of FliC-Nb76 (**B**) interacts with FliC protein (**A**). **C** Analysis of EGFP- FliC-Nb76 protein purification by SDS-PAGE. **D** Determination EGFP- FliC-Nb76 by Western blot. **E** Observation of *S.* Enteritidis and EGFP-FliC-Nb-76 Binding under Laser Confocal Microscopy. **F** Motility analysis of *S.* Enteritidis on 0.4% agar LB plate by treatment with BSA and FliC-Nb76. **G** Observation of *S.* Enteritidis flagella treated with BSA and FliC-Nb76 under electron microscopy. **H** Statistical analysis of the movement areas of clinical resistant S. Enteritidis strains by treatment with FliC-Nb76. **I** Determination of minimum effective concentration of FliC-Nbs to inhibit the motility of *S.* Enteritidis FY-04. **J** Motility analysis of *S.* Enteritidis treated with BSA and FliC-Nb76 under Laser Confocal Microscopy. **K** Movement distance of *S.* Enteritidis treated with BSA and FliC-Nb76

FliC nanobody inhibition of *S.* Enteritidis adhesion to and invasion of HIEC-6, RAW264.7, and chick intestinal epithelial cells

The effects of selected FliC-Nbs on *S.* Enteritidis adhesion to and invasion of HIEC-6 and RAW264.7 cells were investigated. Both the PS (positive serum) group and the FliC-Nb76 group showed significantly reduced adhesion and invasion relative to the NS (negative serum) group after challenge of mCherry S. Enteritidis adhering to HIEC-6 cells (Fig. 3A, B) and RAW264.7 cells (Fig. 3C, D). Fluorescence microscopy showed that pre-treatment with FliC-Nb76 significantly reduced the adhesion of mCherry *S.* Enteritidis to both HIEC-6 (Fig. 3E) and RAW264.7 (Fig. 3F) cells. As analyzed by ImageJ software, the integrated optical density of the FliC-Nb76 group was significantly lower than that of the negative control group (Fig. 3G, H). The number of the mCherry-ZZ64 and mCherry-ZZ77 strains adhering to HIEC-6
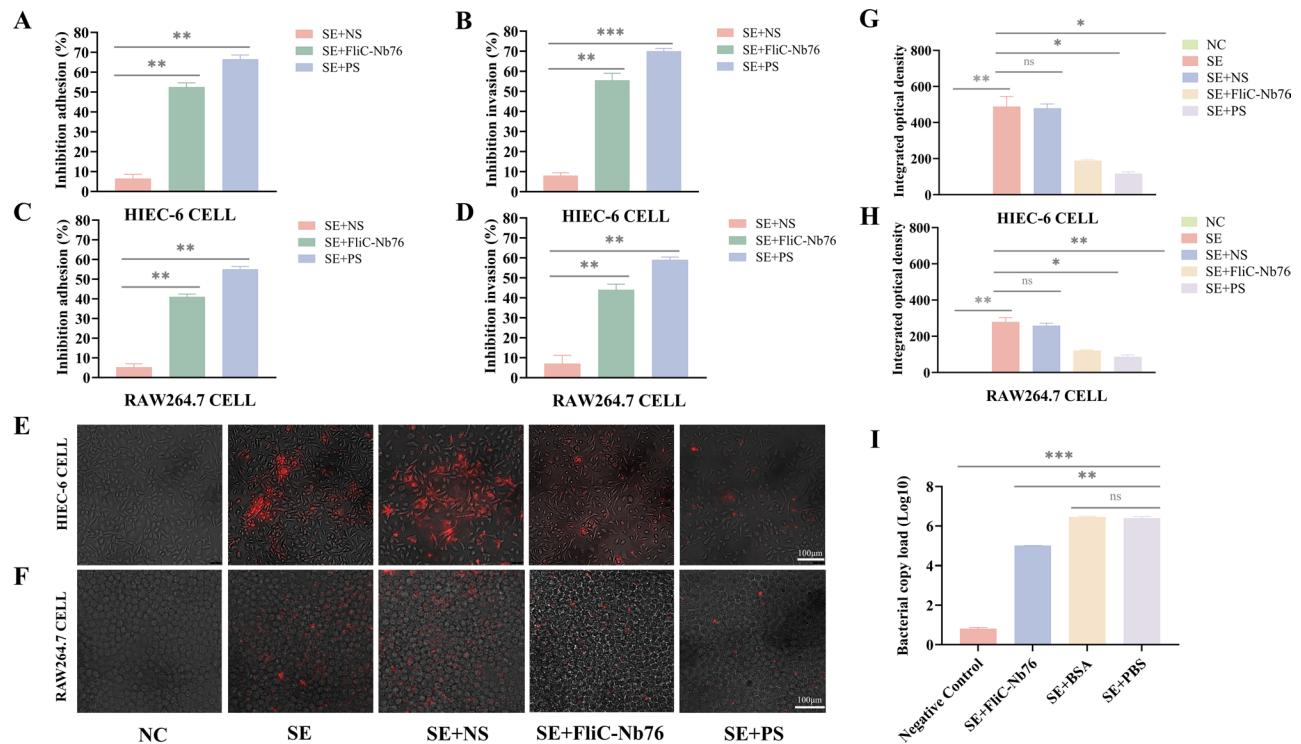
Yang *et al. Journal of Nanobiotechnology*   (2024) 22:629

Page 10 of 16

Fig. 3 Recombinant nanobodies inhibit HIEC-6, RAW264.7 cells and chick intestinal epithelial cells infection by the mCherry *S.* Enteritidis (ATCC13076). **A**, **B** Assessment of HIEC-6 cells adhesion and invasion by *S.* Enteritidis. **C**, **D** Assessment of RAW264.7 cell adhesion and invasion by S. Enteritidis. **E**, **F** mCherry-*S.* Enteritidis (ATCC13076) adheres to HIEC-6 cells and RAW264.7 cells which is inhibited by FliC-Nb76 through fluorescence microscopy observation. **G**, **H** the integrated optical density of mCherry-*S.* Enteritidis (ATCC13076) adheres to HIEC-6 cells and RAW264.7 cells. **I** The inhibitory effect of FliC-Nb76 in chicken intestinal epithelial cells was evaluated using qPCR

and RAW264.7 cells after pretreatment with FliC-Nb76 also decreased significantly. (Fig. S4). The results indicated that FliC-Nb76 could specifically block both adhesion to and invasion of HIEC-6 and RAW264.7 cells by *S.* Enteritidis. This inhibitory effect was also observed in the clinical isolates of drug-resistant *S.* Enteritidis (Fig. S5, 6). The PMD18-T-HilA plasmid (3100 bp) was diluted using a 10-fold dilution gradient. A linear standard curve was established using the logarithm of the copy number of the PMD18-T-HilA plasmid as the X axis and the Cycler value as the Y axis (Fig. S6) The target-gene copy number of *S.* Enteritidis infecting the chick jejunal epithelial cells was determined by qPCR to assess whether FliC-Nb76 could block infection of the cells by *S.* Enteritidis. Conversion of the CT value to the copy number determined by qPCR showed that compared with the PBS and BSA groups the number of target-gene copies of *S.* Enteritidis in jejunal epithelial cells of FliC-Nb76-pretreated groups decreased significantly, indicating a significant reduction in the numbers of *S.* Enteritidis infecting the cells after pretreatment with FliC-Nb76 (Fig. 3I).

Preparation, induced expression, and identification of recombinant *L. lactis* carrying nanobodies

The construction of NZ8148-USP45-LEISSTCDA-FliC-Nb76 was successful (Fig. 4A). The whole-cell ELISA showed that the fusion protein with a His tag could be anchored and expressed in the recombinant NZ9000 strain (Fig. 4B, C). Western blotting also showed that the fusion protein containing the His tag in the induced culture supernatant could react with the anti-His monoclonal antibody (Fig. 4D), indicating the successful expression and secretion of FliC-Nb76 in the recombinant NZ9000 strain. *L. lactis*-VHH were induced by 20 ng/mL Nisin for 4, 6, 8, and 12 h, and the culture supernatants were collected and analyzed using His-tag competitive ELISA. This showed that the absorbance at 450 nm increased significantly in the culture supernatants after FliC-Nb76-NZ9000 induction relative to supernatant with no load, accompanied by greater accumulation of nanobodies as the time of induction, seen in increased absorbances at 450 nm (Fig. 4E). The FliC-Nb76-NZ9000 strain was induced with 20 ng/mL Nisin, and samples were collected at 2, 4, 6, 8, 10, and 12 h for Western blotting. This showed that the His-tagged nanobodies could be observed after 2 h of induction, with the expression increasing gradually after 4 h of induction, and reaching
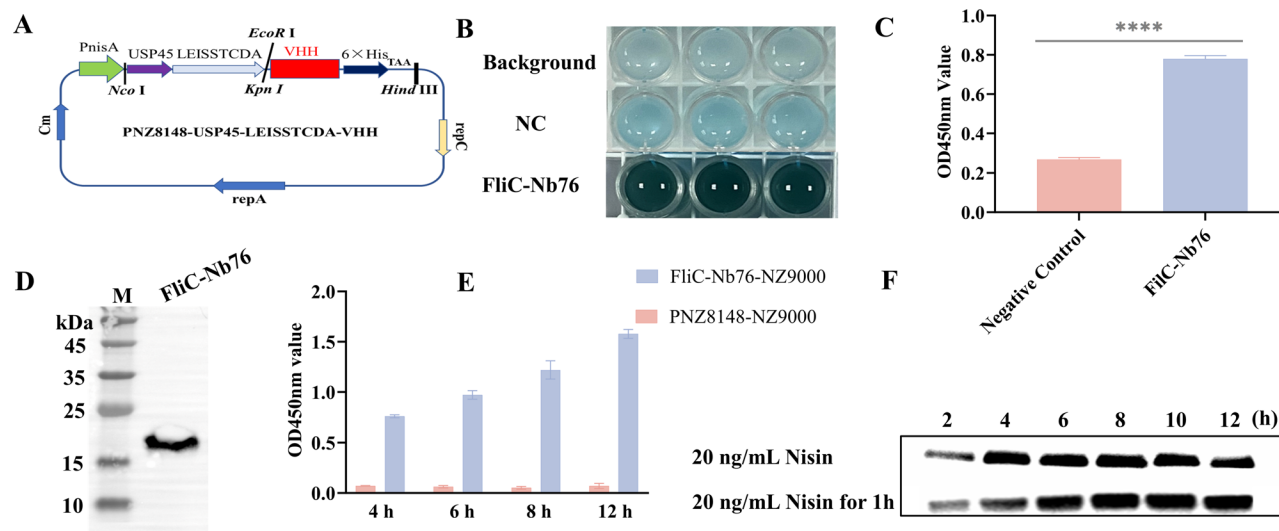
Fig. 4 Preparation, induced expression, identification of recombinant *L. lactis* carrying nanobodies. **A** Schematic diagram of pNZ8148-VHH plasmid. **B** Color change in Whole cell ELISA after adding TMB; darker colors indicate more His-tag fusion proteins. **C** The Whole cell ELISA results were analyzed by OD450nm. **D** The expression of His label fusion protein was identified by Western blot. **E** ELISA identification of the induced FliC-Nb76-NZ9000 supernatant. **F** Analysis of *L. lactis*-VHH expression by the Nisin induction and remove Nisin induction way at different times

a maximum yield at 8 h, after which it remained essentially unchanged. After the removal of Nisin after 1 h of induction, the culture supernatants were collected and analyzed by Western blotting. The concentration of recombinant nanobodies expressed in the FliC-Nb76-NZ9000 strain was determined using His Tag competitive ELISA kit. A four-parameter logistic fitting standard curve was performed based on the His Tag standard protein concentration and the measured OD450nm value (Figure S8). According to the fitting curve, the concentrations of nanobodies secreted by the FliC-Nb76-NZ9000 strain after continuous induction with Nisin for 8 h and cultivation remove Nisin for 8 h were determined as follows: FliC-Nb76-NZ9000 (1.61 µg/mL), FliC-Nb76-NZ9000 (2.39 µg/mL, remove Nisin). This showed that neither Nisin-free culture nor continuous induction using Nisin significantly affected the expression and secretion of the nanobodies (Fig. 4F).

Targeted inhibition of *S.* Enteritidis by *L. lactis* carrying nanobodies in the chick intestine

The scheme of the animal experimental process is shown in Fig. 5A. As shown by PCR, FliC-Nb76-NZ9000 could colonize the intestinal tract (Fig. S7D). Comparison of duodenal, jejunal, and ileal tissue showed that FliC-Nb76-NZ9000 colonized all intestinal segments, with the degree of colonization reducing significantly over time in all segments (Fig. 5B). In the first three days after challenge with *S.* Enteritidis, the mortality rate in the SE group was 26.7% and that in the PNZ8148-NZ9000 group was 13.3%, while no death was observed in the FliC-Nb76-NZ9000 group (Table 3). At the same time, no deaths occurred in any of the experimental groups after the third day of

challenge. The feces collected from each experimental group on days 3 and 7 were analyzed using smear plates. The number of *S.* Enteritidis excreted by the PNZ8148-NZ9000 group was slightly reduced compared to the SE group, but the numbers were significantly decreased in the FliC-Nb76-NZ9000 group (Fig. 5C). On days 3 and 7, duodenal, jejunal, and ileal tissues were collected from each experimental group for qPCR analysis. Compared to the SE group, the copy numbers of *S.* Enteritidis in the different intestinal segments did not change significantly in the PNZ8148-NZ9000 group on either day 3 or day 7. However, in the FliC-Nb76-NZ9000 group, there was a significant decrease in the *S.* Enteritidis copy numbers in all intestinal segments at these time points (Fig. 5D, E). Live imaging of the intestines revealed that, compared to the SE group, the fluorescence intensity of *S.* Enteritidis in the PNZ8148-NZ9000 group was slightly reduced but was significantly decreased in the FliC-Nb76-NZ9000 group (Fig. 5F). Ileal tissue collected from the different experimental groups on day 7 was sectioned and stained with HE. The results showed that FliC-Nb76-NZ9000 effectively inhibited the pathological damage to the ileal epithelial cells caused by *S.* Enteritidis infection (Fig. 5G).

On day 7, RNA was extracted from the intestinal segments of the different experimental groups, and the levels of the cytokines IL-1 β, IL-10, IL-8, TNF-α, and IL-17 A were determined by qPCR (Fig. 6A-E). The results showed that *S.* Enteritidis infection up-regulated the mRNA expression of the pro-inflammatory cytokines IL-1 β, IL-8, TNF-α, and IL-17 A, but there was no significant change in the level of anti-inflammatory cytokine IL-10. Pretreatment with FliC-Nb76-NZ9000 was found to reduce the expression of pro-inflammatory cytokines
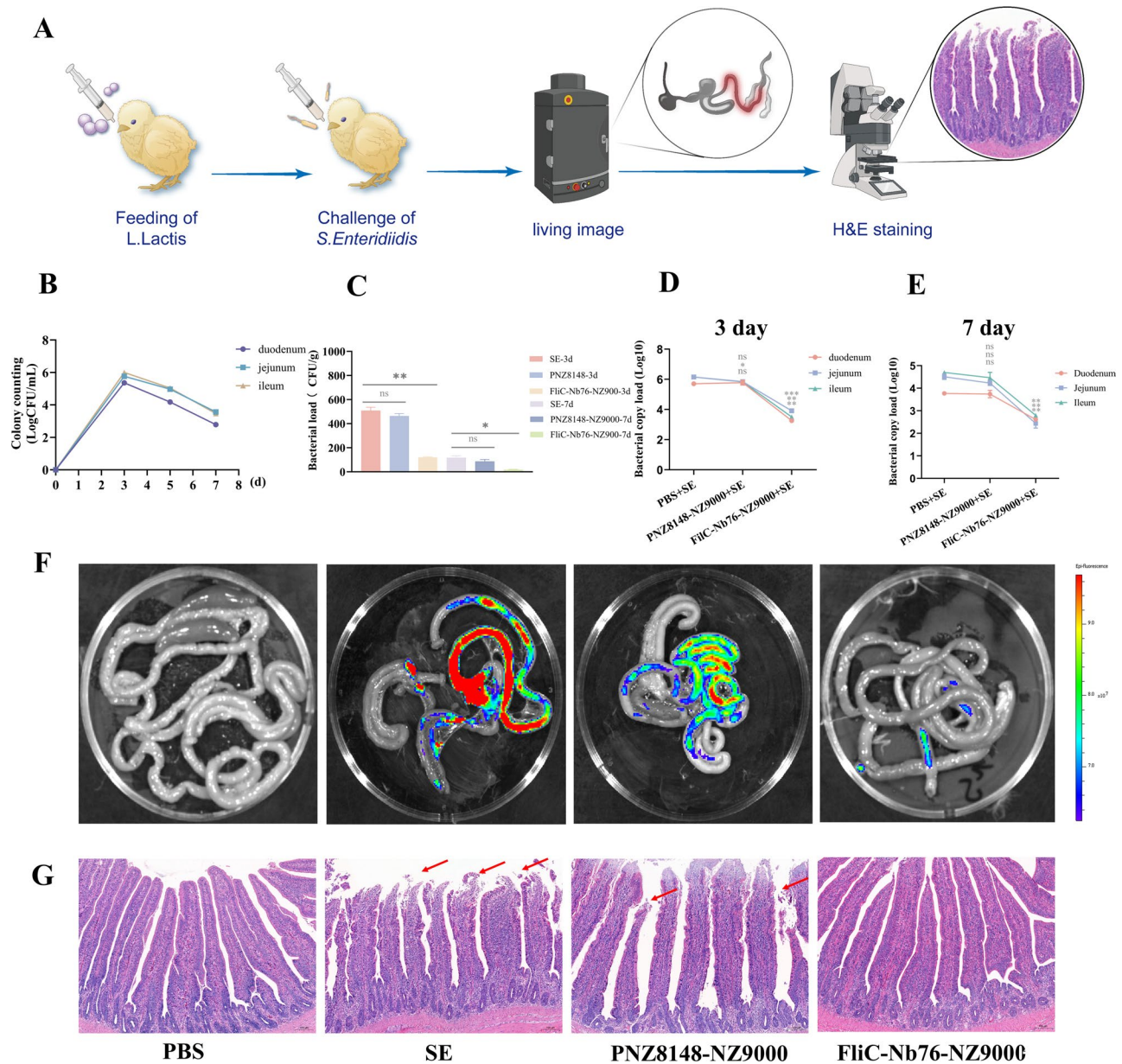
Fig. 5 Determination of targeted inhibition of S. Enteritidis by L. lactis carrying nanobodies in Chicken intestine. **A** Scheme of animal experiment process **B** Plate counting of FliC-Nb76-NZ9000 in duodenum, jejunum, and ileum **C** Count analysis of *S*. Enteritidis in feces on the 3rd and 7th days after *S*. Enteritidis challenged. **D E** The gene copy number of *S*. Enteritidis was detected by qPCR after 3 days and 7 days of challenge with *S*. Enteritidis f Analysis of ileal histopathology at the 7th day after challenge by *S*. Enteritidis. **F** Living image of the intestine at the 7th day after challenge by *S*. Enteritidis. **G** Analysis of ileal histopathology at the 7th day after challenge by *S*. Enteritidis

Table 3 Mortality statistics of chicks after feeding *S*. Enteritidis in each experimental treatment group (3 d)

Group	Lethal dose	Chicks	Dead chicks	Mortality rate
PBS	0	15	0	0
SE	2×10^9CFU	15	4	26.7%
PNZ8148-NZ9000	2×10^9CFU	15	2	13.3%
FilC-Nb76-NZ9000	2×10^9CFU	15	0	0

and promote the up-regulation of the anti-inflammatory IL-10. FliC-Nb76-NZ9000 can thus effectively alleviate the inflammatory response caused by *S*. Enteritidis, thereby reducing the impact and harm of *S. Enteritidis* infection-induced enteritis.

Discussion

According to the data of the World Health Organization (WHO), approximately 1.9 billion people suffer from diarrhea each year, resulting in 715 000 deaths [35].
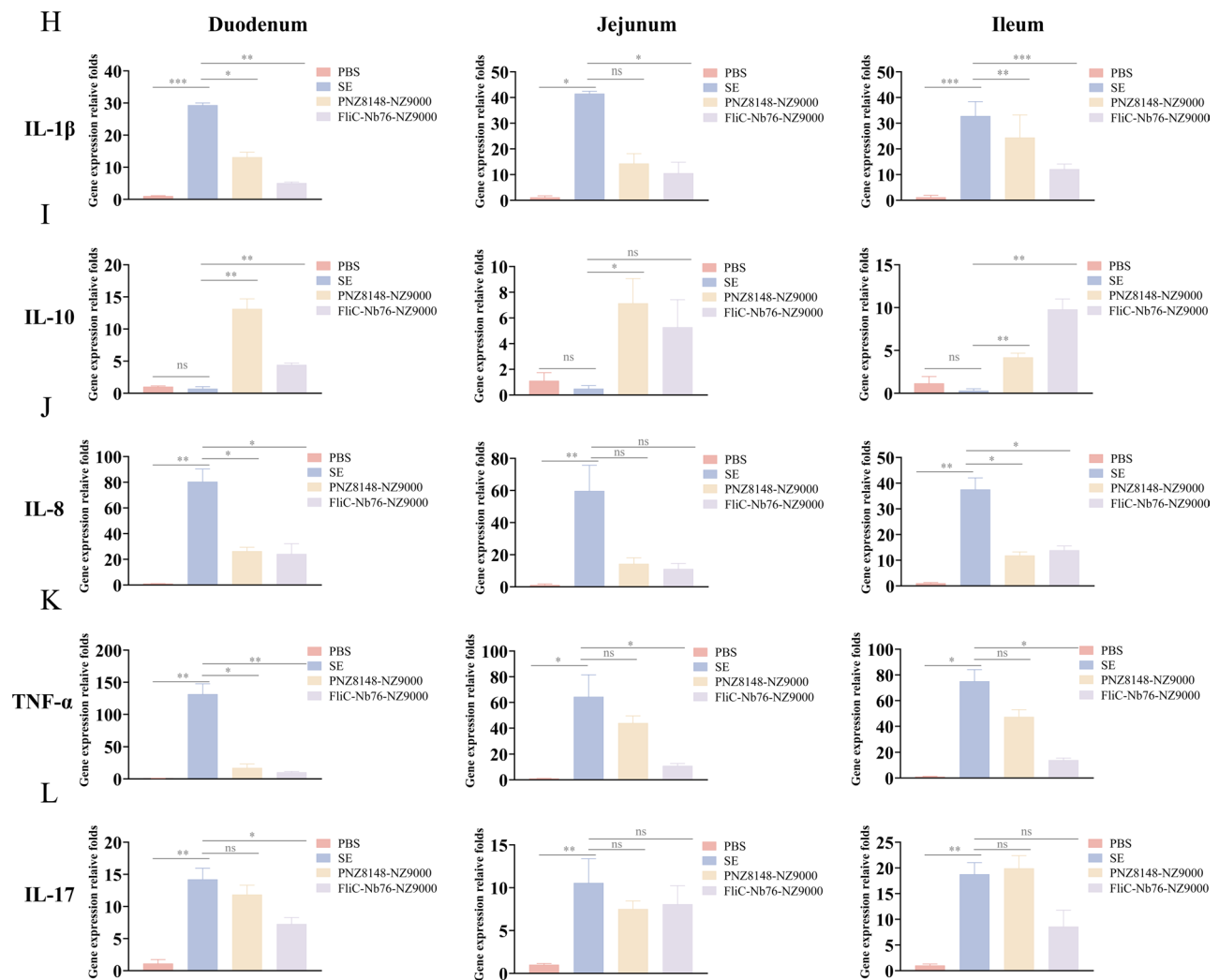
Fig. 6 Differential expression of intestinal inflammatory related cytokines. In the duodenal, jejunal, and ileal segments, compared to the SE group, both PNZ8148-NZ9000 group and FliC-Nb76-NZ9000 group showed **A** a significant decrease in the relative expression levels of IL-1β. **B** a significant decrease in the relative expression levels of IL-10, **C** a significant decrease in the relative expression levels of IL-8, **D** a significant decrease in the relative expression levels of TNFα in the duodenal, jejunal, and ileal tissues, **E** a significant decrease in the relative expression levels of IL-17 in the duodenal, jejunal tissues and a significant decrease in the relative expression in FliC-Nb76-NZ9000group ileal tissues but a slight increase in PNZ8148-NZ9000 group ileal tissues

One-third of these cases are attributed to foodborne illnesses. Among various foodborne pathogens, *Salmonella* is one of the most common causative agents. Research has shown that *Salmonella* contamination of poultry products accounts for 50% [2] of *Salmonella* outbreak incidents, and consumption of *Salmonella*-contaminated eggs may be one of the main causes of human foodborne *Salmonella* gastrointestinal disease. The Centers for Disease Control and Prevention (CDC) in the USA consider antibiotic-resistant *Salmonella* a serious public health threat [36]. In developed countries, *Salmonella* resistance is primarily caused by the use of antibiotics in animal husbandry [37]. Based on available statistics from the USA, *Salmonella* shows the highest resistance to streptomycin (11.2%), tetracycline (10.4%), sulfamethoxazole (9.4%), and ampicillin (9.1%), followed by chloramphenicol

(4.0%), nalidixic acid (3.5%), ceftriaxone (2.4%), cefoxitin (2.2%), amoxicillin-clavulanate (2.1%), gentamicin (1.4%), trimethoprim-sulfamethoxazole (1.3%), ciprofloxacin (0.4%), and azithromycin (0.1%) [38]. Therefore, there is an urgent need to develop alternatives to these antibiotics or identify effective treatment strategies to address the issue of antibiotic resistance in *Salmonella*.

Nanobodies, with their high sensitivity and specificity, are important members of the antibody family and have widespread applications in both neutralizing and treating bacterial infections [39]. *L. lactis* is able to express exogenous proteins as delivery vectors, as well as having the probiotic ability to colonize the intestine, and is widely utilized in biomedical research, animal husbandry, and disease prevention and control [40]. In one study, the pNZ8112 plasmid was used to construct

LNZ9000-rTGEV-SN, a recombinant *L. lactis* expressing the N-terminal domain of the S protein of transmissible gastrointestinal virus (TGEV). This recombinant *L. lactis* was used for oral immunization of BALB/c mice, resulting in a localized mucosal immune response against TGEV. The induced antibodies were also able to prevent TGEV infection, indicating that recombinant *L. lactis* could be a valuable tool for the future development of vaccines against TGEV [41]. Additionally, a vaccine based on mucosal injection of recombinant *L. lactis* secreting *Brucella* copper-zinc superoxide dismutase (SOD) was found to contribute to the control of brucellosis [42]. *L. lactis* is able to colonize the intestine. The effectiveness of *L. lactis* carrying neutralizing nanobodies depends both on the colonization efficiency and the numbers of nanobodies secreted. The present study conducted a preliminary exploration of the effects of FliC-Nb76-NZ9000 in the chick intestine. It was found that FliC-Nb76-NZ9000 colonized the duodenum, jejunum, and ileum to different extents. It was also found that FliC-Nb76-NZ9000 could regulate the inflammatory response caused by *S.* Enteritidis. Fecal excretion of *S.* Enteritidis was reduced, together with damage to the intestinal villous epithelium. It may also contribute to the recovery from damage caused by this self-limiting pathogen, *S.* Enteritidis. Meanwhile, studies have shown that oral administration of enrofloxacin to chicks can disrupt the normal barrier function of the intestine, thereby promoting the infection and colonization of *S.* Enteritidis in the intestine [43]. The feeding of enrofloxacin can also have adverse effects on the gut microbiota and metabolic profile, hindering recovery from *S.* Enteritidis infection [44]. However, using probiotics as the carrier system for FliC-Nb76 nanobodies eliminates concerns about such issues. *L. lactis* is a microbial factory bacterium that has been widely used in both scientific research and fermentation engineering. It is anticipated that in the near future, it will be applied in more industries, effectively promoting the development of biomedical research, animal husbandry, and disease prevention and control.

This study proposes a strategy for the delivery of nanobodies to the intestinal tract, and showed that nanobodies can effectively inhibit *S.* Enteritidis colonization of the intestine, reduce inflammation caused by *S.* Enteritidis, and minimize its damage to the intestinal tract. The findings provide a new approach for the treatment of *S.* Enteritidis infection in chicks and offers new insights for the prevention and treatment of drug-resistant bacterial infections. However, this study pays less attention to the homology of FliC [45], and further research and exploration into the cross-protective efficacy against other types of *Salmonella* invasion is warranted. Additionally, the nanobodies carried by *L. lactis* can be reasonably modified, such as being engineered into bivalent or multivalent antibodies to enhance their efficacy [46].

Conclusion

This study found that FliC-Nb76 inhibited the motility of *S.* Enteritidis and effectively blocked both *S.* Enteritidis adhesion to and invasion of HIEC-6 and RAW264.7 cells. On this basis, *L. lactis* was used for carrying *S.* Enteritidis-neutralizing nanobodies. The *L. actis*-VHH was found to inhibit the colonization of *S.* Enteritidis and reduce inflammation and minimize intestinal damage in the chick intestines. These results provide a new strategy for the treatment of drug-resistant *S.* Enteritidis infection in the intestinal tracts of chicks.

Supplementary Information

The online version contains supplementary material available at https://doi.org/10.1186/s12951-024-02904-8.

Supplementary Material 1

Data availability
No datasets were generated or analysed during the current study.

Declarations

Ethics approval and consent to participate
Ethics approval and consent to participate. All experimental animals were approved by the Animal Ethics Committee (AEC) of the College of Life Sciences, Sichuan University (License: SYXK (Chuan) 2013–185). All experimental procedures and animal care strictly followed the guidelines of Animal Management of Sichuan University. Consent for publication Not applicable.

Consent for publication
We confirm that all authors have read and agreed to the manuscript before submission.

Competing interests
The authors declare no competing interests.

Author details
[1]Animal Disease Prevention and Food Safety Key Laboratory of Sichuan Province, Key Laboratory of Bio-Resource and Eco-Environment of

Ministry of Education, College of Life Sciences, Sichuan University, Chengdu, Sichuan, China

²Key Laboratory of Bio-Resource and Eco-Environment of Ministry of Education, College of Life Sciences, Sichuan University, Chengdu, Sichuan, People's Republic of China

³School of Pharmacy and Bioengineering, Chongqing University of Technology, Chongqing 400054, China

⁴National Engineering Research Center for Biomaterials, Sichuan University, Chengdu, Sichuan, People's Republic of China

References

1. Carroll LM, Buehler AJ, Gaballa A, Siler JD, Cummings KJ, Cheng RA, Wiedmann M. Monitoring the microevolution of *Salmonella* enterica in healthy dairy cattle populations at the individual farm level using whole-genome cequencing. Front Microbiol. 2021;12:763669.
2. Li S, He Y, Mann DA, Deng X. Global spread of *Salmonella* enteritidis via centralized sourcing and international trade of poultry breeding stocks. Nat Commun. 2021;12:5109.
3. Bell SC, Mall MA, Gutierrez H, Macek M, Madge S, Davies JC, Burgel PR, Tullis E, Castaños C, Castellani C, et al. Global burden of bacterial antimicrobial resistance in 2019: a systematic analysis. Lancet (London England). 2022;399:629–55.
4. Qin S, Xiao W, Zhou C, Pu Q, Deng X, Lan L, Liang H, Song X, Wu M. Pseudomonas aeruginosa: pathogenesis, virulence factors, antibiotic resistance, interaction with host, technology advances and emerging therapeutics. Signal Transduct Target Ther. 2022;7:199.
5. Li W, Han H, Liu J, Ke B, Zhan L, Yang X, Tan D, Yu B, Huo X, Ma X, et al. Antimicrobial resistance profiles of *Salmonella* isolates from human diarrhea cases in China: an eight-year surveillance study. One Health Adv. 2023;1:2.
6. Clokie MRJ, Sicheritz-Pontén TE. Phage therapy: insights from the past, the great need of the present, and glimpses into the future. Phage (New Rochelle). 2022;3:65–6.
7. Lim Y-M, Vadivelu J, Mariappan V, Venkatraman G, Vellasamy KM. Effective therapeutic options for melioidosis: antibiotics versus phage therapy. Pathogens. 2023;12:11.
8. Sawa T, Kinoshita M, Inoue K, Ohara J, Moriyama K. Immunoglobulin for treating bacterial infections: one more mechanism of action. Antibodies. 2019;8:52.
9. Chen Y, Duan W, Xu L, Li G, Wan Y, Li H. Nanobody-based label-free photoelectrochemical immunoassay for highly sensitive detection of SARS-CoV-2 spike protein. Anal Chim Acta. 2022;1211:339904.
10. Chi X, Zhang X, Pan S, Yu Y, Shi Y, Lin T, Duan H, Liu X, Chen W, Yang X, et al. An ultrapotent RBD-targeted biparatopic nanobody neutralizes broad SARS-CoV-2 variants. Signal Transduct Target Ther. 2022;7:44.
11. Hanke L, Das H, Sheward DJ, Perez Vidakovics L, Urgard E, Moliner-Morro A, Kim C, Karl V, Pankow A, Smith NL, et al. A bispecific monomeric nanobody induces spike trimer dimers and neutralizes SARS-CoV-2 in vivo. Nat Commun. 2022;13:155.
12. Li Q, Humphries F, Girardin RC, Wallace A, Ejemel M, Amcheslavsky A, McMahon CT, Schiller ZA, Ma Z, Cruz J, et al. Mucosal nanobody IgA as inhalable and affordable prophylactic and therapeutic treatment against SARS-CoV-2 and emerging variants. Front Immunol. 2022;13:995412.
13. Lu Z, Liu Z, Li X, Qin X, Hong H, Zhou Z, Pieters RJ, Shi J, Wu Z. Nanobody-based bispecific neutralizer for Shiga toxin-producing *E. Coli*. ACS Infect Dis. 2022;8:321–9.
14. Wang P, Yu G, Wei J, Liao X, Zhang Y, Ren Y, Zhang C, Wang Y, Zhang D, Wang J, Wang Y. A single thiolated-phage displayed nanobody-based biosensor for label-free detection of foodborne pathogen. J Hazard Mater. 2023;443:130157.
15. Wang Y, Mei Y, Ao Z, Chen Y, Jiang Y, Chen X, Qi R, Fu B, Tang J, Fang M, et al. A broad-spectrum nanobody targeting the C-terminus of the hepatitis B surface antigen for chronic hepatitis B infection therapy. Antiviral Res. 2022;199:105265.
16. Virdi V, Palaci J, Laukens B, Ryckaert S, Cox E, Vanderbeke E, Depicker A, Callewaert N. Yeast-secreted, dried and food-admixed monomeric IgA prevents gastrointestinal infection in a piglet model. Nat Biotechnol. 2019;37:527–30.
17. Barta ML, Shearer JP, Arizmendi O, Tremblay JM, Mehzabeen N, Zheng Q, Battaile KP, Lovell S, Tzipori S, Picking WD, et al. Single-domain antibodies pinpoint potential targets within Shigella invasion plasmid antigen D of the needle tip complex for inhibition of type III secretion. J Biol Chem. 2017;292:16677–87.
18. Ebrahimizadeh W, Mousavi Gargari S, Rajabibazl M, Safaee Ardekani L, Zare H, Bakherad H. Isolation and characterization of protective anti-LPS nanobody against *V.* Cholerae O1 recognizing Inaba and Ogawa serotypes. Appl Microbiol Biotechnol. 2013;97:4457–66.
19. Vanmarsenille C, Díaz Del Olmo I, Elseviers J, Hassanzadeh Ghassabeh G, Moonens K, Vertommen D, Martel A, Haesebrouck F, Pasmans F, Hernalsteens JP, De Greve H. Nanobodies targeting conserved epitopes on the major outer membrane protein of *Campylobacter* as potential tools for control of Campylobacter colonization. Vet Res. 2017;48:86.
20. Chevance FF, Hughes KT. Coordinating assembly of a bacterial macromolecular machine. Nat Rev Microbiol. 2008;6:455–65.
21. Evans LD, Hughes C, Fraser GM. Building a flagellum outside the bacterial cell. Trends Microbiol. 2014;22:566–72.
22. Elhadad D, Desai P, Rahav G, McClelland M, Gal-Mor O. Flagellin is required for host cell invasion and normal *Salmonella* pathogenicity island 1 expression by Salmonella enterica Serovar Paratyphi A. Infect Immun. 2015;83:3355–68.
23. Salehi S, Howe K, Lawrence ML, Brooks JP, Bailey RH, Karsi A. *Salmonella* enterica serovar kentucky flagella are required for broiler skin adhesion and Caco-2 cell invasion. Appl Environ Microbiol. 2017;83:e02115–02116.
24. Riazi A, Strong PC, Coleman R, Chen W, Hirama T, van Faassen H, Henry M, Logan SM, Szymanski CM, Mackenzie R, Ghahroudi MA. Pentavalent single-domain antibodies reduce Campylobacter jejuni motility and colonization in chickens. PLoS ONE. 2013;8:e83928.
25. Schumacher D, Helma J, Schneider AFL, Leonhardt H, Hackenberger CPR. Nanobodies: chemical functionalization strategies and intracellular applications. Angew Chem Int Ed Engl. 2018;57:2314–33.
26. Qiao W, Liu F, Wan X, Qiao Y, Li R, Wu Z, Saris PEJ, Xu H, Qiao M. Genomic features and construction of streamlined genome chassis of Nisin Z producer *Lactococcus lactis* N8. *Microorganisms* 2022, 10:47.
27. Andersen KK, Marcotte H, Álvarez B, Boyaka PN, Hammarström L. In situ gastrointestinal protection against anthrax edema toxin by single-chain antibody fragment producing lactobacilli. BMC Biotechnol. 2011;11:126.
28. Wang Z, Yu Q, Fu J, Liang J, Yang Q. Immune responses of chickens inoculated with recombinant *Lactobacillus* expressing the haemagglutinin of the avian influenza virus. J Appl Microbiol. 2013;115:1269–77.
29. De Angelis M, Gobbetti M. Environmental stress responses in *Lactobacillus*: a review. Proteomics. 2004;4:106–22.
30. Gu K, Song Z, Zhou C, Ma P, Li C, Lu Z, Liao Z, Huang Z, Tang Y, Li H, et al. Development of nanobody-horseradish peroxidase-based sandwich ELISA to detect *Salmonella* enteritidis in milk and in vivo colonization in chicken. J Nanobiotechnol. 2022;20:167.
31. Khani MH, Bagheri M, Zahmatkesh A, Aghaiypour K, Mirjalili A. Effect of flagellin on inhibition of infectious mechanisms by activating opsonization and *Salmonella* flagellum disruption. Microb Pathog. 2020;142:104057.
32. Spöring I, Felgner S, Preuße M, Eckweiler D, Rohde M, Häussler S, Weiss S, Erhardt M. Regulation of flagellum biosynthesis in response to cell envelope stress in *Salmonella* enterica serovar typhimurium. mBio. 2018;9. https://doi.org/10.1128/mbio.00736–00717.
33. Lin KH, Hsu AP, Shien JH, Chang TJ, Liao JW, Chen JR, Lin CF, Hsu WL. Avian reovirus sigma C enhances the mucosal and systemic immune responses elicited by antigen-conjugated lactic acid bacteria. Vaccine. 2012;30:5019–29.
34. Zeng Z, Yu R, Zuo F, Zhang B, Ma H, Chen S. Recombinant *Lactococcus lactis* expressing bioactive exendin-4 to promote insulin secretion and beta-cell proliferation in vitro. Appl Microbiol Biotechnol. 2017;101:7177–86.
35. Besser JM. *Salmonella* epidemioaogy: A whirlwind of change. Food Microbiol. 2018;71:55–9.
36. Solomon SL, Oliver KB. Antibiotic resistance threats in the United States: stepping back from the brink. Am Family Phys. 2014;89:938–41.
37. Anderson AD, Nelson JM, Rossiter S, Angulo FJ. Public health consequences of use of antimicrobial agents in food animals in the United States. Microb Drug Resist (Larchmont NY). 2003;9:373–9.
38. McDermott PF, Zhao S, Tate H. Antimicrobial resistance in nontyphoidal *Salmonella*. Microbiol Spectr. 2018;6. https://doi.org/10.1128/microbiolspec.arba-0014-2017.
39. Qin Q, Liu H, He W, Guo Y, Zhang J, She J, Zheng F, Zhang S, Muyldermans S, Wen Y. Single domain antibody application in bacterial infection diagnosis and neutralization. Front Immunol. 2022;13:1014377.

40. Song AA-L, In LLA, Lim SHE, Rahim RA. A review on *Lactococcus lactis*: from food to factory. Microb Cell Fact. 2017;16:55.
41. Tang L, Li Y. Oral immunization of mice with recombinant *Lactococcus lactis* expressing porcine transmissible gastroenteritis virus spike glycoprotein. Virus Genes. 2009;39:238–45.
42. Sáez D, Fernández P, Rivera A, Andrews E, Oñate A. Oral immunization of mice with recombinant *Lactococcus lactis* expressing Cu,Zn superoxide dismutase of Brucella abortus triggers protective immunity. Vaccine. 2012;30:1283–90.
43. Mei X, Ma B, Zhai X, Zhang A, Lei C, Zuo L, Yang X, Zhou C, Wang H. Florfenicol enhances colonization of a *Salmonella* enterica serovar enteritidis floR mutant with major alterations to the intestinal microbiota and metabolome in neonatal chickens. Appl Environ Microbiol. 2021;87:e0168121.
44. Ma B, Mei X, Lei C, Li C, Gao Y, Kong L, Zhai X, Wang H. Enrofloxacin shifts intestinal microbiota and metabolic profiling and hinders recovery from *Salmonella* enterica subsp. Enterica serovar typhimurium infection in neonatal chickens. mSphere. 2020;5. https://doi.org/10.1128/msphere.00725–00720.
45. Huen J, Yan Z, Iwashkiw J, Dubey S, Gimenez MC, Ortiz ME, Patel SV, Jones MD, Riazi A, Terebiznik M, et al. A novel single domain antibody targeting FliC flagellin of *Salmonella* enterica for effective inhibition of host cell invasion. Front Microbiol. 2019;10:2665.
46. Vandenbroucke K, de Haard H, Beirnaert E, Dreier T, Lauwereys M, Huyck L, Van Huysse J, Demetter P, Steidler L, Remaut E, et al. Orally administered *L. Lactis* secreting an anti-TNF nanobody demonstrate efficacy in chronic colitis. Mucosal Immunol. 2010;3:49–56.

Publisher's note

Springer Nature remains neutral with regard to jurisdictional claims in published maps and institutional affiliations.